J. Coat. Technol. Res., **16** (6) 1597–1607, 2019
https://doi.org/10.1007/s11998-019-00251-0

Film formation and crosslinking of waterborne two-component coatings containing quaternized ammonium groups

Silfredo Javier Bohorquez, Dirk Mestach

Abstract A study was done to investigate the crosslinking and film formation of a waterborne two-component system consisting of an aqueous epoxy functional dispersion and tertiary amine functional polymer dispersions. Techniques used were Fourier transform infrared, atomic force microscopy, environmental scanning electron microscopy, dynamic mechanical thermal analysis, and energy-dispersive X-ray spectroscopy. Next to covalent crosslinking, it was also demonstrated that the crosslinks, containing quaternized ammonium groups, cluster together to form ''nest-like'' structures in the bulk of the crosslinked film.

Keywords Film formation, Isocyanate-free crosslinking, Emulsion polymers, Epoxy amine system

Introduction

Waterborne two-component polyurethane coatings have been commercially available for the last 25 years. Over the years, much progress has been made to improve the final properties of these coatings, but because the crosslinking reaction depends on the reaction of aqueous polyols with emulsified or dispersed polyisocyanates, the formation of surface defects that arise from the reaction of isocyanate with water is still a concern. Furthermore, polyisocyanate crosslinkers are under scrutiny from legislators, so their longer-term use might become an issue.[1,2] Around the same time as the launch of waterborne two-component polyurethanes, allnex introduced an isocyanate-free binder system onto the market.[3] The system was based on an epoxy functional polymer dispersion (component A) made by means of emulsion polymerization that was combined with a secondary emulsion of an acrylic polymer carrying both carboxylic acid and tertiary amine functional groups (component B). The secondary emulsion is made by conventional solution polymerization followed by emulsification and distillation of the organic solvent. The crosslinking reactions occurring after mixing both components A and B were studied by van der Ven et al.[4] using ^{1}H-NMR on low molecular weight model compounds and consisted of the following reactions:

Esterification	Epoxy + acid → ester
Polycondensation	Epoxy + epoxy → poly(ether)
Etherification	Epoxy + hydroxyl → ether
Quaternization	Epoxy + tert.-amine → quaternized ammonium (OH counter-ion)
	Epoxy + tert.-amine + carboxylic acid → quaternized ammonium ($R\text{-}COO^{\ominus}$ counter-ion)
	Epoxy + tert.-amine + epoxy → polyether
Salt formation	tert.-amine + carboxylic acid → ammonium salt
Hydrolysis	Epoxy + water → diol

It was proven that the quaternization reactions were predominant, so in the network, the polymer chains were linked by quaternized ammonium groups, giving the polymer film a cationic character (Fig. 1).

This first-generation binder system offered reasonable performance and is currently being used exten-

This paper was presented at the 2018 European Technical Coatings Congress on June 26–29, 2018, in Amsterdam, The Netherlands.

S. J. Bohorquez (✉), D. Mestach
Allnex Netherlands BV, Synthesebaan 1, 4612 RB Bergen op Zoom, The Netherlands
e-mail: silfredo.bohorquez@allnex.com

sively in both metal- and wood-coating applications. In wood-primer applications, the cationic sites prevent extractables in the wood from bleeding through the coating. Some significant drawbacks of the tert.-amine functional secondary emulsion used are high production cost and limited stability, and pot-life after mixing the A and B components. Therefore, a study was performed to investigate if component B could also be made by means of emulsion polymerization. The parameters of the thus obtained polymer dispersion, such as molecular weight, particle size, T_g, and functionality on the film formation and crosslinking kinetics were studied. In this paper, the crosslinking kinetics are discussed together with the mode of film formation.

Experimental methods and materials

Methyl methacrylate, n-butyl acrylate, methacrylic acid, styrene, and dimethylaminoethyl methacrylate were used as received. SETAQUA® 8455 and SETAQUA® 8556 are, respectively, tert.-amine and epoxy functional dispersions, obtained from Allnex Netherlands BV. The properties of SETAQUA 8455 are given in Table 3. In the text this dispersion will be referred to as ''reference.'' The properties of SETAQUA® 8556 are as follows: solid content 50%, pH 8.5, and epoxy equivalent weight 621 (g/Eq).

Synthesis of amino-functionalized dispersions by means of emulsion polymerization

The method to prepare the tert.-amino-functionalized waterborne dispersions (''TAFD'') using emulsion polymerization was described elsewhere.[5] The pot-life for this two-component system was extended by locating the tert.-amino groups at the inside of the particles, and screening them by an anionic steric barrier. A long pot-life is advantageous in industrial situations where the formulation needs to be stable for a longer period of time after blending of the components. Therefore, the synthesis is a two-step process. In the first step a polymeric stabilizer is made by means of emulsion polymerization using a chain transfer agent. The monomers used are given in Table 1.

The number average molecular weight of the first polymer was approximately 17,000 g/mole. The pH of the first polymer was raised to a value of about 9 using aqueous ammonia. In the second step, a variable monomer composition was polymerized in the presence of the neutralized first polymer. Compositions of the second polymer are given in Table 2.

The ratio of the first phase polymer to the second phase polymer is 1:1. Figure 2 gives a schematic illustration for the sequential polymerization.

The properties of the synthesized prototype dispersions are given in Table 3. The main difference between the prototypes (TAFD 1 to TAFD 3) is the concentration of the DMAEMA in the polymer. In order to make a comparison between the three TAFD, a commercial dispersion, SETAQUA® 8445 (allnex), made by secondary emulsification, and described elsewhere,[6] was used.

The average particle diameter dp was determined by dynamic light scattering using the Zetasizer® model S90. Solid content (S.C.) was determined gravimetrically according to ISO 3251. The minimum film formation temperature was measured according to ASTM D2354-10.

Table 1: First-phase monomers

Monomer	Percentage
Methyl methacrylate	49
Butyl acrylate	43
Methacrylic acid	8

Table 2: Second-phase monomers

	TAFD 1 (%)	TAFD 2 (%)	TAFD 3 (%)
Methyl methacrylate	58	56	54
n-Butyl acrylate	25	24	23
Styrene	8	8	8
Dimethylaminoethyl methacrylate	8	12	15

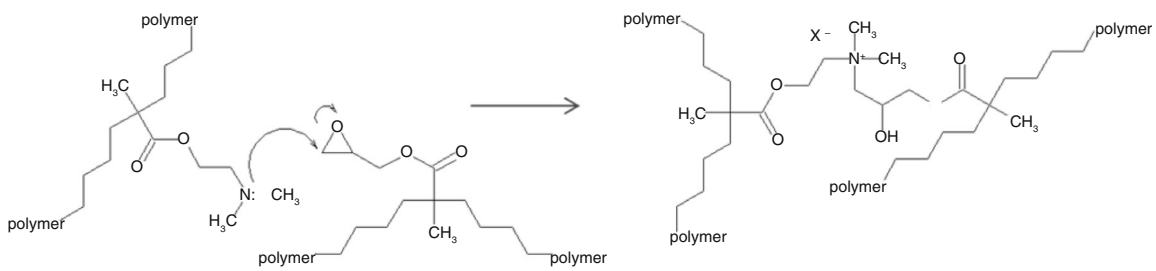

Fig. 1: Crosslink. Counter-ion X^- is OH^- or COO^-

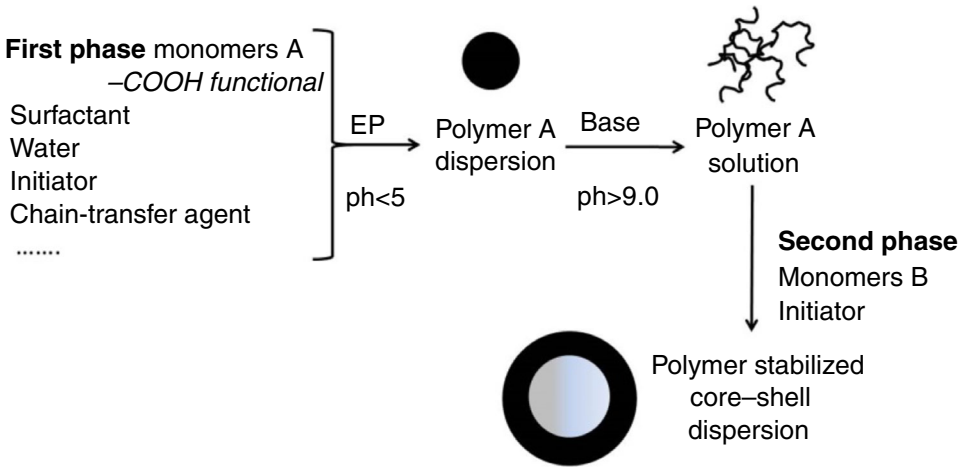

Fig. 2: Schematic representation of the synthesis of TAFD

Table 3: Properties of tert.-amine functional dispersions

Experiment	dp (nm)	S.C. (%)	pH	MFFT (°C)	NH eq. weight (g/Eq)
TAFD 1	52	31	9.1	13	290
TAFD 2	56	34	9.1	23	330
TAFD 3	64	37	9.1	31	350
SETAQUA® 8445	175	36	9.7	n. a.	655

Characterization of nonpigmented films

Films were cast from the combination of various TAFD (component A) with the epoxy functional dispersion SETAQUA® 8556 (component B). The mechanical properties of these coatings after film formation were measured using dynamic mechanical thermal analysis (DMTA) with a DMA-Q800 apparatus. König hardness was measured after applying a film on glass (100 μm wet layer thickness according to ASTM D4366-16). The films were dried at 23°C and 45% relative humidity (RH) for 24 h. Chemical resistance was determined using a spot test on films applied at a wet film thickness of 125 μm on Leneta® cards. The films were dried at 23°C and 45% RH for 24 h. Spots of different chemicals were applied on the film surface, and the damage was evaluated visually immediately after removing the stain. The reaction of amino groups in component A with epoxy groups in component B during film formation was followed by FTIR using a Nicolet 380 spectrophotometer. A drop containing a blend of waterborne epoxy dispersion blended with the different tert.-amino functional prototypes (and the commercial reference) was dried for 24 h at room temperature, recording a spectrum at set intervals. The disappearance of the epoxy signal was used to calculate conversion.

Film formation study using scanning electronic microscopy

Micrographs were obtained using a Quanta® 250 FEG ESEM (FEI, Netherlands) equipped with a Peltier cooling stage and a gaseous secondary electron detector (GSED). An aluminum stub of 10 mm in diameter and a height of 5 mm covered with mica was used as a substrate. To obtain monolayer coverage of polymer particles on the substrate, the latex was diluted with water to 0.1 wt% solid content. A drop of the diluted latex was placed onto the substrate which was mounted on the Peltier cooling stage using a eutectic metal alloy (Fusible Alloy 47, INNOVATOR Sp. Zo. o.) with a low melting temperature (47°C) in order to ensure a

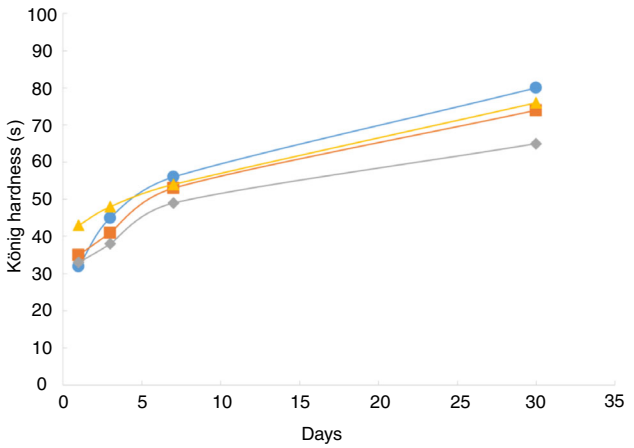

Fig. 3: Hardness development for the nonpigmented coatings as a function of drying time (blue: reference, orange: TAFD 1, gray: TAFD 2, yellow: TAFD 3)

good heat conductance. The sample was placed in the chamber at a pressure of 270 Pa. Water vapor was used to create pressure inside the chamber, and thus, the start-up humidity in the proximity of the sample was 42%. The pressure was kept constant during the experiment. Images were taken at different locations on the sample for each temperature step. The imaging conditions of the microscope were as follows: accelerating voltage 5 kV, spot size 3, and working distance 6.8 mm, GSE detector (500 mm). A Quantax 70 spectrophotometer coupled to the ESEM was employed to determine the atom composition of the film surface through energy-dispersive X-ray spectroscopy.

Results and discussion

Film performance and crosslinking kinetics

Nonpigmented coatings were prepared by blending the prototype TAFD 1–3 with the epoxy functional waterborne dispersion SETAQUA 8556. The ratio between the two components was such that equivalent amounts of tert.-amino and epoxy would react. As coalescing agent, 2.5 wt% of butyldiglycol was added to the blend.

Figure 3 shows the increase in hardness as a function of time for different TAFD compared to the reference. It can be noticed that for the first 7 days, there was hardly any difference in the evolution of the hardness. However, after 30 days, the reference, TAFD 1, and TAFD 3 have higher hardness.

A number of chemical resistance tests were carried out on the nonpigmented coatings. The results are presented in Table 4.

All of the coatings had good water resistance. The prototypes, however, performed worse than the reference for ethanol (48% aqueous) and coffee resistance. This could be an indication of a lower crosslink density in the dried nonpigmented coatings. DMTA was used to determine the extent of crosslinking of the prototypes vs the reference system. Figure 4 shows the DMTA comparison of the reference vs TAFD 3.

Figure 4 reveals that even though the prototype was made by sequential polymerization and hence consisted of two polymer phases, during film formation both phases inter-diffuse as there can only be one T_g observed. Moreover, despite the slight differences in T_g, it is clear that TAFD 3 has a lower crosslink density compared to the reference. The reference shows a sharper increase in storage modulus (after the rubber region) compared to TAFD 3.

The kinetics of the quaternization reaction during film formation was followed by means of FTIR. The disappearance of the oxirane stretching (950 cm^{-1}) of the epoxy dispersion was used to determine the extent of conversion. The drying was evaluated by following the disappearance of the OH stretch and OH scissors due to the evaporation of water from the coating. An example of this is shown in Fig. 5 for the blend of the reference with stoichiometric amounts of epoxy dispersion.

The epoxy conversion and water evaporation during film formation for the reference and prototype 3 are

Table 4: Chemical resistance properties and pot-life of the nonpigmented coatings

Experiment	Water resistance (4-h exposure)	48% Ethanol (6-h exposure)	Coffee (6-h exposure)	Pot-life (days after mixing)
TAFD 1	4	1.5	1.5	> 7
TAFD 2	4	1.5	1.5	> 7
TAFD 3	4.5	2	2	> 7
Reference	5	3.5	3.5	3

(1 = film is damaged; 5 = film is not affected)

shown in Figs. 6 and 7, respectively. For the reference, it can be seen that the system started to react immediately as the water started to evaporate. At 100 min the water was completely evaporated and the system reached approximately 90% conversion. This was totally different for TAFD 3 where the speed of oxirane consumption was much slower. At 100 min water was almost completely evaporated from the coating; however, conversion only reached 40%. These results in combination with DMTA confirmed the

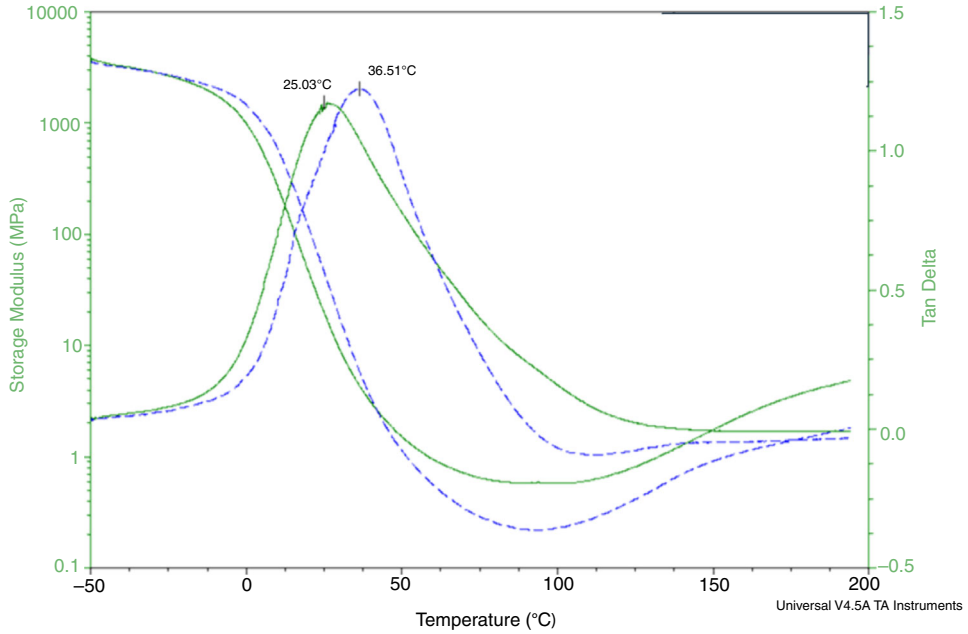

Fig. 4: DMTA on films of nonpigmented coatings: reference (full line) vs TAFD 3 (dotted line)

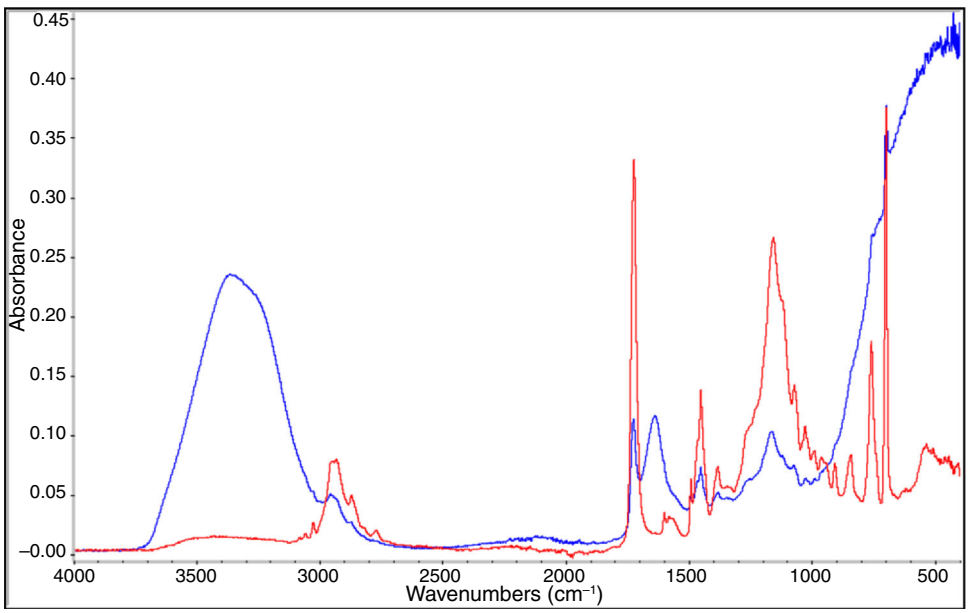

Fig. 5: FTIR spectra of time 0 h (blue) and time 24 h (red) for the reference system (Color figure online)

lower crosslinking density of the TAFD. This was also reflected in the overall worse chemical resistance properties.

Even though the reference and TAFD 3 had the same concentration of DMAEMA in the polymer, the epoxy conversion was quite different. The reason for this can be attributed to differences in film formation. The coalescence of particles from components A and B during the film formation was better for the reference system than for the prototypes. Moreover, in the reference systems the tert.-amine groups come into contact with epoxy groups immediately after the film has been applied, as due to phase inversion of the secondary emulsion, the amino groups are more easily accessible. In the TAFD inter-diffusion of the polymer chains in the component A and B particles proceeds to a lesser extent as the tert.-amine groups are located in the center of the particle.

A series of additional experiments were performed with the aim to redesign the tert.-amino functional dispersion polymer in order to improve the film formation process. Some of the parameters varied were T_g and molecular weight of the first and second phases. It is well known that T_g and molecular weight have a large influence on the mobility of polymer chain that directly affects inter-diffusion during particle–particle coalescence.[7–10] After a series of chemical resistance testing the best TAFD was selected and was compared to TAFD 3 given in Table 5. The performance of the new prototype, TAFD 4, was similar to that of the commercial reference. It is important to mention that TAFD 4 contained 2–4 wt% chain transfer agents in the core phase, which could improve the mobility the polymer chains during the particle–particle coalescence process. The last probably contributed to the lower MFT presented by TAFD 4. The concentration of chain transfer agents was 0% for prototypes TAFD 1–3; therefore, the molecular weight of these prototypes was higher as compared to TAFD 4. In Fig. 8 it is clear that for TAFD 4 the oxirane signal disappearance was similar to that of the reference system. Interestingly, TAFD 4 retained the same long pot-life as for TAFD 3.

Film microstructure analysis by ESEM

In order to further study the differences of the film formation process between the newer TAFD and the reference secondary emulsion, the surface and the cross-sectional topology were analyzed using ESEM. Figure 9 shows the film cross section obtained by ESEM of nonpigmented coatings based on reference, TAFD 3, and TAFD 4. In all cases, the presence of structures that phase-separate from the bulk of the polymer matrix, probably due to a difference in

Table 5: Characteristics of prototypes 3 and 4

Experiment	dp (nm)	S.C. (%)	pH	MFFT (°C)	NH eq. weight (g/Eq)
TAFD 4	150	40	9.1	5	350
TAFD 3	64	37	9.1	31	350

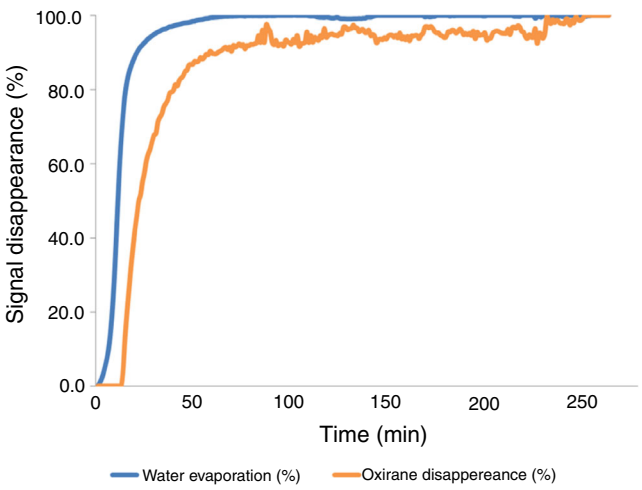

Fig. 6: Epoxy conversion and water evaporation during film formation of the reference system

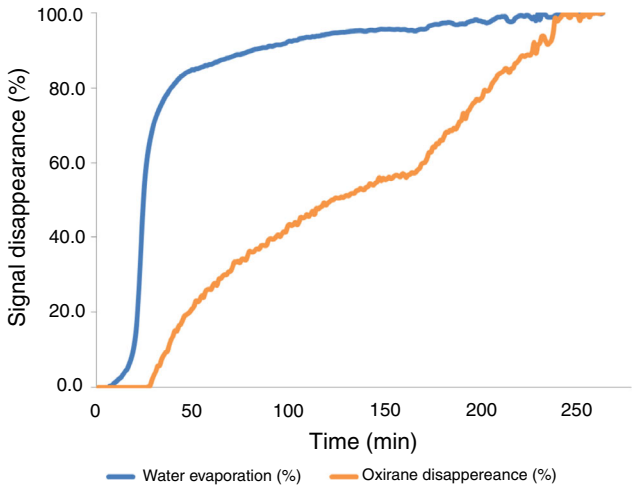

Fig. 7: Epoxy conversion and water evaporation during film formation of TAFD 3

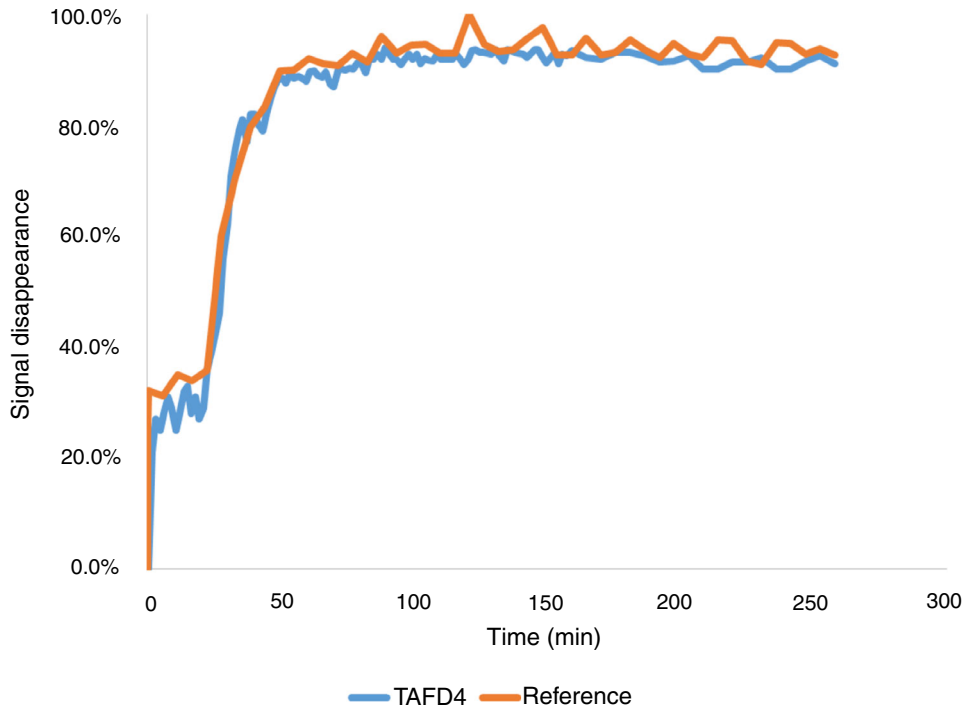

Fig. 8: Comparison of the epoxy conversion between TAFD 4 and the reference system

polarity, can be noted. In this paper these structures will be referred to as ''clusters.'' In Fig. 9, it can be seen that the clusters are scattered in the polymer matrix for the film using the reference dispersion, in the bottom of the film for TAFD 3 and preferably in the upper part of the film for TAFD 4. It is not clear what could be the mechanisms driving the location of such clusters. From the FTIR data, it is known that for the case of TAFD 3 the reaction between tert.-amino and epoxy groups occurs at later stages of the coalescence process; therefore, the quaternized clusters were presumably formed later as well. A large portion of the water usually evaporates preferably from the film surface[11,12]; therefore, the bottom of the film particles could coalesce later. Figure 7 reveals that the system reacted at later stages of the film formation process, likely when more than 90% of the water had evaporated. Figure 8 shows that TAFD 4 and the reference had similar kinetic performance and hence the clusters could have formed in a similar fashion, following previous hypothesis. This was not the case, because for TAFD 4, most of the clusters could be found in the upper part of the film.

Figure 10 shows an example of the clusters found in the reference, TAFD 3, and TAFD 4. It is possible to see that for TAFD 3 the cluster and film formation was limited as it is possible to see noncoalesced polymer particles. More ''nest''-like clusters are found in the case of the reference and TAFD 4. While the filaments forming those clusters differed in their shape, needle-like for the reference and feather-like for TAFD 4, these clusters could also form physical barriers in combination with a chemical barrier (because of the presence of quaternized ammonium groups) against tannins, as demonstrated previously.[13]

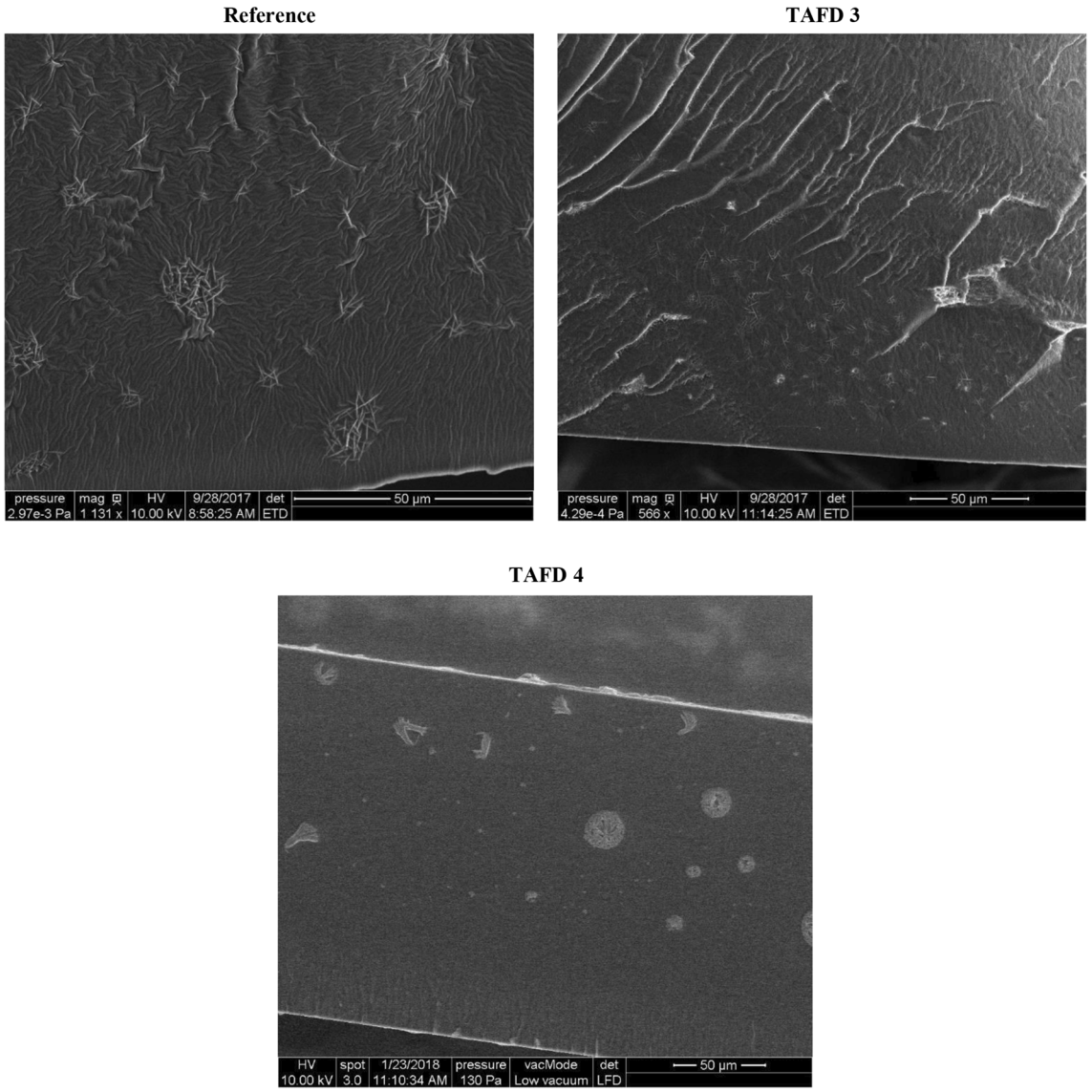

Fig. 9: ESEM film cross-sectional images (only for the reference, the lower part of the picture is actually the upper part of the film)

Energy-dispersive X-ray spectroscopy in combination with the ESEM was used to evaluate the chemical composition of such clusters. Results are shown in Fig. 10. The high concentration of nitrogen indicated that these clusters could be the product of the quaternization process during the crosslinking reaction. It is worth mentioning that the overall composition of the polymer matrix was much lower in nitrogen as compared to the composition in the clusters (Fig. 11).

Conclusions

Conventional emulsion polymerization was used to produce film-forming tert.-amino functional aqueous dispersions. These dispersions were formulated into nonpigmented coatings and evaluated against a reference binder made by secondary emulsification. The evaluation of the kinetic mechanisms of the tert.-amino epoxy reaction during film formation showed that an excellent coalescence of both tert.-amino functional

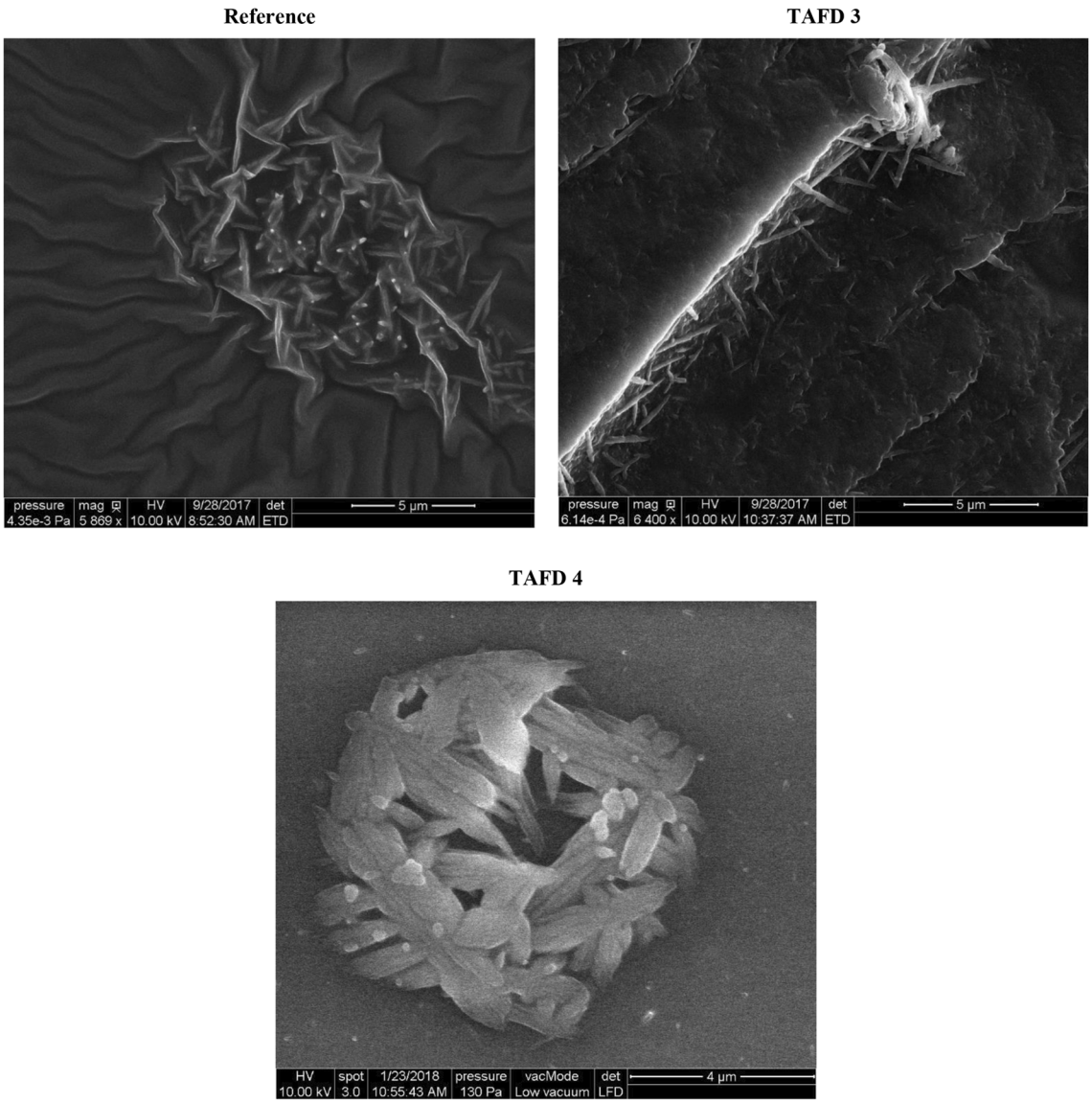

Fig. 10: ESEM images of quaternized polymer clusters

and epoxy functional particles must occur in order to obtain high conversion leading to further crosslinking. If this does not happen, the water drying front could move faster and the reaction occurs at later stages as revealed for TAFD 3, which had poor chemical resistance. Optimization parameters investigated were molecular weight, T_g, and particle size. This has led to TAFD with better film-forming properties such as TAFD 4.

The ESEM film cross-sectional analysis revealed the presence of clusters that phase-separated from the polymer matrix. These ''nest''-like clusters were proven to be enriched in nitrogen, as measured by energy-dispersive X-ray spectroscopy in combination with the ESEM, making it likely that they could be the product of the quaternization reaction occurring during the crosslinking.

The presence of these clusters is an interesting finding because this shows the quaternized ammonium groups also form a physical barrier. This phenomenon was not observed until now and gives more insight into how the mechanism for preventing wood and tannin bleeding and chemical attack actually works. It was clear that an enrichment of such clusters at the film surface was beneficial for the performance of these two-component nonisocyanate coating systems.

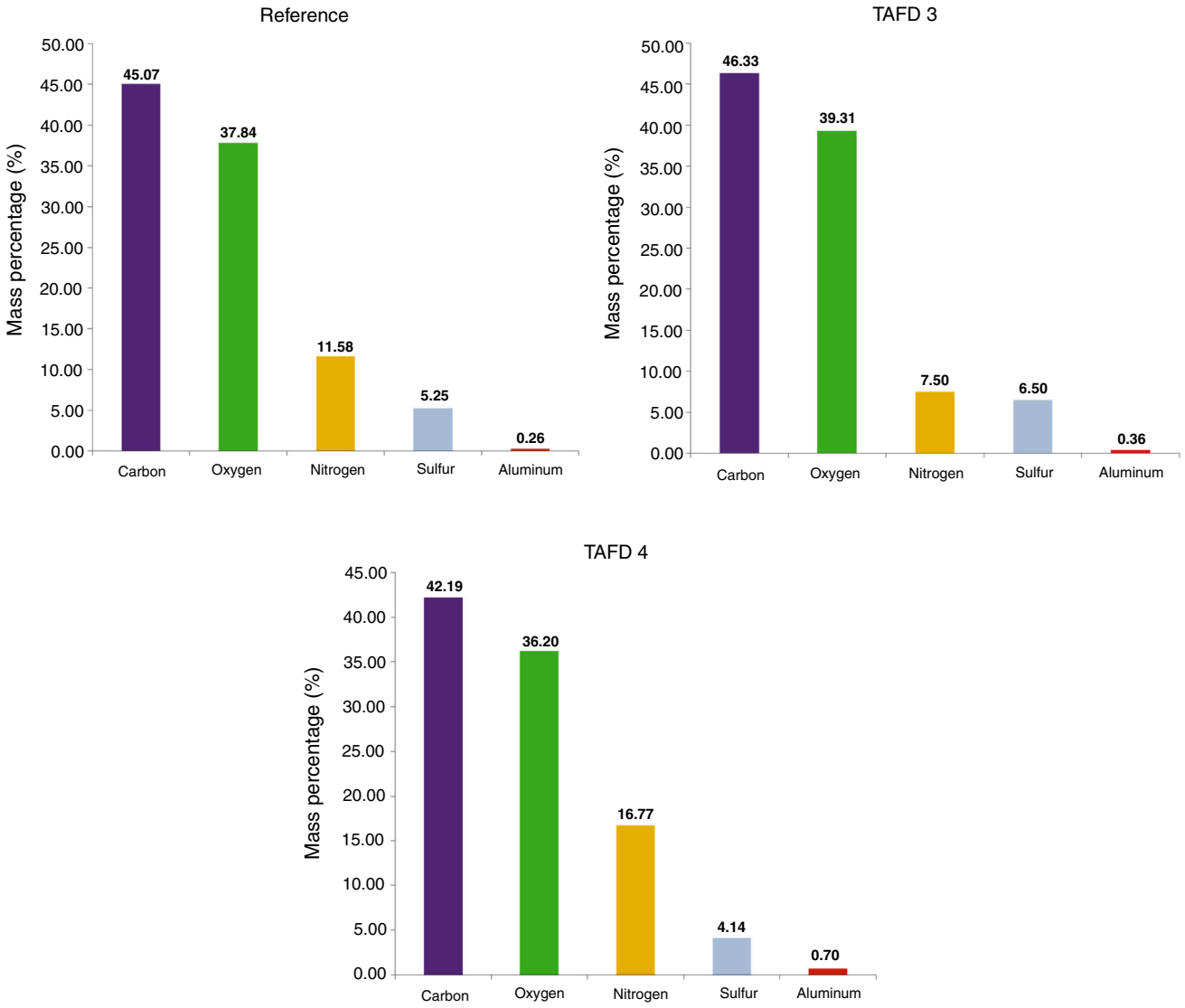

Fig. 11: Chemical composition of quaternized polymer clusters

References

1. Morgan, CJ, Haworth, AE, "Allergic Contact Dermatitis from 1,6-Hexamethylene Diisocyanate in a Domestic Setting." *Contact Dermat.*, **48** 224 (2003)
2. Pedata, P, Corvino, AR, Lamberti, M, "Non Pulmonary Effects of Isocyanates." In: Otsuki, T (ed.) *Allergy and Immunotoxicology in Occupational Health (Current Topics in Environmental Health and Preventive Medicine)*, pp. 129–141. Springer, Berlin (2017)
3. Brinkman, E, Vandevoorde, P, "Waterborne Two-Pack Isocyanate-Free Systems for Industrial Coatings." *Prog. Org. Coat.*, **34** (1–4) 21–25 (1998)
4. Van der Ven, LGJ, Leijzer, RTM, Brinkman, E, "Curing Mechanism and Film Properties of Water-Borne Isocyanate-Free All-Acrylic Coatings." *Double Liaison Science et Techniques*, **448–449** 67–71 (1999)
5. Bohorquez, S, Mestach, D, "Amine Functional Anionic Polymer Dispersion and Coating Compositions Thereof" WO2017191131A1
6. Mestach, D, Esser, R, Ligtenberg, J, Dolphijn, P, "A New Waterborne Binder for Preventing Knot-Bleeding" *Proceedings European Coatings Congress*, April 2013
7. Winnik, M, "Latex Film Formation." *Curr. Opin. Colloid Interface Sci.*, **2** (2) 192–199 (1997)
8. Sambasivam, M, Klein, A, Sperling, LH, "Healing and Fracture Studies in Incompletely Annealed Latex Films and Related Materials" In: *ACS Symposium Series*, *Film Formation in Waterborne Coatings,* Chapter 11, pp 179–199, American Chemical Society (1996)
9. Kan, CS, "Role of Particle Size on Latex Deformation During Film Formation." *J. Coat. Technol.*, **71** 89–95 (1999)
10. Eckersley, ST, Rudin, A, "Film Formation of Acrylic Copolymer Latices: A Model of Stage II Film Formation"

In: *ACS Symposium Series Film Formation in Waterborne Coatings,* Chapter 1, pp 2–21
11. Sperry, PR, Snyder, BS, O'Dowd, ML, Lesko, PM, ''Role of Water in Particle Deformation and Compaction in Latex Film Formation.'' *Langmuir*, **10** (8) 2619–2628 (1994)
12. Carter, FT, Radoslaw Kowalczyk, M, Millichamp, I, Chainey, M, Keddie, JL, ''Correlating Particle Deformation with Water Concentration Profiles During Latex Film Formation: Reasons That Softer Latex Films Take Longer to Dry.'' *Langmuir*, **30** (32) 9672–9681 (2014)
13. Wiedenhoeft, A, ''Understanding Extractive Bleed.'' *Coat. Technol.*, **10** (3) 48–53 (2010)